Study of the influence of the motion limit of a horizontal single-axis tracker on the annual incident energy in a PV power plant

Arsenio Barbón
Department of Electric Engineering
University of Oviedo
Gijón, Spain
barbon@uniovi.es

Covadonga Bayón-Cueli
DNV UK Limited
OPEX, Aberdeen, UK
covadonga.bayon.cueli@dnv.com

Luis Bayón
Department of Mathematics
University of Oviedo
Gijón, Spain
bayon@uniovi.es

Verónica Carreira-Fontao
Polytechnic School of Engineering of Gijón
University of Oviedo, Gijón, Spain
carreirafontao@gmail.com

2024 IEEE International Conference on Environment and Electrical Engineering and 2024 IEEE Industrial and Commercial Power Systems Europe (EEEIC / I&CPS Europe) | 979-8-3503-5518-5/24/$31.00 ©2024 IEEE | DOI: 10.1109/EEEIC/ICPSEUROPE61470.2024.10751286

***Abstract*—This paper analyses the influence of the motion limit of a horizontal single-axis tracker on the incident energy on the PV field. The Miraflores PV power plant (Spain) is analysed. As most of the PV power plants in Spain have a motion limit of ± 60 (^{o}) (so-called actual scenario). A Mathematica© code has been implemented to calculate the annual incident energy and the daily incident energy in the PV field. The proposed assessment indicator is the annual incident energy ratio with respect to the actual scenario. The maximum annual incident energy corresponds to the actual scenario, but the reduction of the motion limit does not imply excessive energy losses. For $\beta_{\max} = \pm 55(^\circ)$ this loss is 0.050%. The $\beta_{\max} = \pm 55(^\circ)$ scenario slightly favours the diffuse component and the actual scenario favours the beam component. Therefore, at a location where the diffuse component predominates, the actual scenario may not be optimal.**

***Index Terms*—Single-axis tracker, Limit of motion, Annual incident energy rate.**

I. Introduction

The European Union (EU) has promoted the decarbonisation of the energy sector through the transition to the use of renewable energy in this sector [1]. Wind and solar energy are the best positioned. The International Energy Agency (IEA) forecasts are very good for photovoltaic (PV) technology, as this type of energy will play a key role in electricity generation over the next decade [2]. The continued reduction in the levelised cost of energy ($LCOE$) of this technology is one of the most notable reasons [3]. The energy generated by PV technology worldwide was 1291 (TWh) in 2022 [2]. It is estimated to be 5405 (TWh) in 2030 [2].

PV technologies are classified according to the number of rotational motions around an axis: 2 motions (dual-axis tracker), 1 motion (single-axis tracker), and no rotational motion. Dual-axis tracking systems generate the most electrical power [4], although maintenance costs are higher [5]. Single-axis trackers, on the other hand, generate less electrical power [4], but have lower maintenance costs [6]. Therefore, single-axis trackers are currently the most widely used [6]. Specifically the horizontal single-axis tracker (horizontal north-south axis and east-west tracking) [6]. The study of this tracker will be the focus of this paper.

A large number of parameters are involved in the design of a photovoltaic plant: the available surface area, the shape and orography of the land, the pitch, the minimum E-W distance between two adjacent mounting systems, the length of a mounting system, the limit of the tracker's motion, etc. This paper focuses on the energetic study of the influence of the motion limit of a horizontal single-axis tracker, which in locations with significant wind loads is a fundamental factor. Most PV power plants in Spain have a motion limit of ± 60 (^{o}).

The main contributions of this research can be synthesised in the following proposals: (i) A study of the effect of the motion limit of a horizontal single-axis tracker on the annual incident solar irradiation on the PV field; (ii) A study of the effect of the motion limit of a single-axis horizontal tracker on the daily solar irradiation incident on the photovoltaic field; (iii) A detailed analysis of how the motion limit of a single-axis horizontal tracker affects the components of the incident solar irradiance.

II. Governing equations

A. Periods of operation of a horizontal single-axis tracking

A horizontal single-axis tracker has three periods of operation [7]: (i) normal tracking mode, (ii) backtracking mode and (iii) limited range of motion.

On each day, most of the time, a horizontal single-axis tracker operates in normal tracking mode, i.e. following the daily movement of the Sun. In this period of operation the PV modules rotate from east to west. The astronomical solar algorithm governing the normal tracking mode maximises the solar irradiance incident on the PV field. To do so, this algorithm seeks to minimise the angle formed by the solar ray and the normal to the PV module [8]. The tilt angle (β) governing this period of operation can be calculated from the equation [8]:

$$\beta = \theta_t = \arctan(\tan \theta_z \, |\sin \gamma_s|) \tag{1}$$

where θ_t is the solar transversal angle (^{o}), θ_z is the zenith angle of the Sun (^{o}), and γ_s is the azimuth of the Sun (^{o})

Due to the detrimental effects of shading between PV modules (occurrence of hot spots [9], deterioration of the PV module), solar tracking algorithms focus on avoiding shading between them. At sunrise and sunset, conditions are ideal for shadows to develop between the PV modules. To avoid this phenomenon, the solar algorithm employs a technique called backtracking [10]. The aim of the backtracking mode is to avoid shading between PV modules, but without obtaining the maximum incidence solar irradiance. The angle governing the backtraking mode is β_B and is given by the following equation [7]:

$$\beta_B = \theta_t - \arccos\left(\frac{e_t}{W}\cos\theta_t\right) \tag{2}$$

where θ_t is the solar transversal angle (^{o}), e_t is the pich (m), W is the width of a mounting system (m).

Like other solar trackers, this solar tracker has a limited range of motion. This range is normally $\beta_{\max} = \pm 60$ (^{o}) [6]. The wind loads determine the choice of this angle.

The tilt angles β, β_B, and $\beta_{\max}$ influence the incident solar irradiance on the PV field.

B. Incident solar irradiance on the photovoltaic field

Knowing independently each of the three components that form the incident solar irradiance on the PV field will be important in this study. The incident solar irradiance on the PV field can be determined by the well-known equation (3) [8]:

$$\begin{aligned} &I_t\left(n,T,\beta,\gamma\right) = \\ &\quad I_{bh}\left(n,T\right)\cdot\frac{\cos\theta_i}{\cos\theta_z} + I_{dh}\left(n,T\right)\cdot\left(\frac{1+\cos\beta}{2}\right) + \\ &\quad + \left(I_{bh}\left(n,T\right) + I_{dh}\left(n,T\right)\right)\cdot\rho_g\cdot\left(\frac{1-\cos\beta}{2}\right) \end{aligned} \tag{3}$$

where $I_t(n,T,\beta,\gamma)$ is the total incident solar irradiance on the PV field (W/m^2), I_{bh} is the horizontal beam irradiance characterised by its strong dependence on the location of the PV plant (W/m^2), I_{dh} is the horizontal difusse irradiance characterised by its strong dependence on the location of the PV plant (W/m^2), θ_i is the incident angle in each operating period (^{o}), θ_z is the zenith angle of the Sun (^{o}), β is the tilt angle in each operating period (^{o}), γ is the azimuth angle (^{o}), and ρ_g is the ground reflectance (0.2 is commonly adopted when the ground characteristics are unknown) (dimensionless).

In the determination of I_{bh} and I_{dh} the particular meteorological conditions of the PV plant must be taken into account. For this purpose, the procedure presented by [11] has been used for their determination due to: accuracy, easy applicability, and use in different climates [4].

Equations (4), (5) and (6) can be used to determine the incident angle θ_i in each operating period:

- Normal tracking mode [8]:

$$\cos\theta_i = \sqrt{\cos^2\theta_z + \cos^2\delta\sin^2\omega} \tag{4}$$

where δ is the solar declination (^{o}), and ω is the hour angle (^{o}).

- Backtracking mode [7]:

$$\cos\theta_i = \cos\beta_B\cos\theta_z + \sin\beta_B\sin\theta_z\cos\left(\gamma_s - \gamma\right) \tag{5}$$

- Limited range of motion [7]:

$$\cos\theta_i = \cos\beta_{\max}\cos\theta_z + \sin\beta_{\max}\sin\theta_z\cos\left(\gamma_s - \gamma\right) \tag{6}$$

From a cost-effectiveness point of view, it is necessary to know the incident energy in the PV field. The following equation was used for this purpose:

$$H_t\left(n,\beta\right) = \int_{T_R(n)}^{T_S(n)} I_t(n,T,\beta)dT \tag{7}$$

where H_t is the incident solar irradiation on the PV field (Wh/m^2), n is the day of the year (day), and T is the solar time (h), T_R is the sunrise (h), and T_S is the sunset (h).

C. Annual incident energy rate

The concept of annual incident energy rate ($AIER$) is commonly used to evaluate the influence of different parameters in PV systems [12]. In this study, which analyses the influence of the motion limit of a horizontal single-axis tracker, the following equation is proposed:

$$AIER = \frac{AIE_*}{AIE_{60}} \tag{8}$$

where the subscript $*$ represents the annual incident energy on the PV field with a limit of motion of $\beta^*_{\max}$ (± 50 to ± 59 (^{o})), and the subscript 60 represents the value of the annual incident energy on the PV field with a limit of motion of ± 60 (^{o}).

III. Results and discussion

In this section, the influence of the motion limit of a horizontal single-axis tracker on the annual incident energy on the PV field in an active PV power plant will be analysed. The Miraflores PV power plant is located in Castuera, Extremadura (Spain). Its geographical and technical data are listed in Table I. A range of movement limits between ± 50 (^{o}) and ± 60 (^{o}) was investigated. The ± 60 (^{o}) movement limit of the Miraflores PV power plant will be referred to as the actual scenario. An important aspect of this study is that the beam and diffuse solar irradiances on the horizontal surface under meteorological conditions of the PV power plant have been taken into account using the methodology presented by [11] and the PVGIS database [13].

Table I. Specifications of Miraflores PV power plant.

Specifications	
Latitude	$38°46'4.8''N$
Longitude	$5°32'49.2''N$
Altitude (m)	389
Power (MWp)	22
PV modules number	41122
PV module model	LR5-72HBD 535 (LONGI)
PV module dim.(mm)	2256 x 1133
Rotation angle	$\beta_{\max} = \pm 60(°)$
Pitch (m)	6500
Ground reflectance	0.2

A. Annual incident energy on the PV field

Fig. 1 shows the annual incident energy for the limits of motion of a horizontal single-axis tracker under study. This figure shows that the maximum annual incident energy corresponds to the actual scenario.

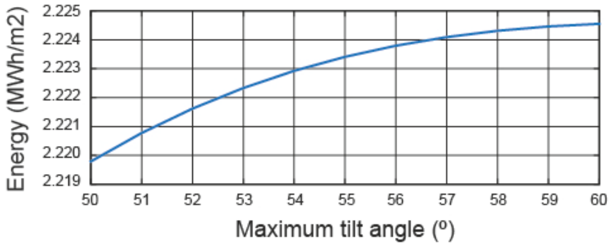

Fig. 1. Annual incident energy versus movement limit.

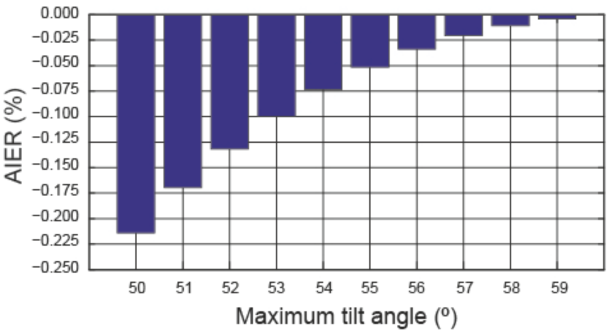

Fig. 2. Annual incident energy ratio.

B. *Annual incident energy ratio*

The annual incident energy ratio for the limits of motion of a single-axis horizontal tracker under study are shown in Fig. 2. According to this figure, for motion limits less than or equal to ± 53 $(^o)$ there are losses with respect to the actual scenario of more than -0.100%. On the other hand, for motion limits greater than or equal to ± 54 $(^o)$, losses with respect to the actual scenario are less than -0.075%. The maximum value of energy losses with respect to the actual scenario is obtained for ± 50 $(^o)$ and is -0.2140%. For a motion limit of ± 55 $(^o)$, energy losses of -0.050% are obtained. It can be concluded that if the wind loads are high at the location of the PV plant, the limit of motion of the horizontal single-axis trackers can be reduced without excessive energy losses.

C. *Daily incident energy loss*

Next, the daily analysis shall be carried out. For this purpose, the daily incident energy of the actual scenario and the daily incident energy for the motion limit of ± 55 $(^o)$ will be subtracted. Fig. 3 represents these results. On every day of the year, the actual scenario achieves better results. This is most noticeable in the summer months. Fig. 4 shows the position of the PV modules for the scenarios $\beta_{\max} = \pm 55(^\circ)$ (blue line) and for $\beta_{\max} = \pm 60(^\circ)$ (actual scenario) (red line) on 21 June (n=172). It can be seen that, in most of the hours, the two profiles overlap, therefore, the incident solar irradiance on the PV modules is the same in these overlapping hours. The difference in the two profiles lies in the waiting time at the position of the motion limit. In the $\beta_{\max} = \pm 55(^\circ)$ scenario (blue line) this time is longer than in the actual scenario (red line). This is the period to be analysed. Fig. 5 represents only the beam component in the actual scenario (red line) and in the scenario $\beta_{\max} = \pm 55(^\circ)$ (blue line). As can be seen, the current scenario performs better. This is due to the behaviour of cos θ_i. Fig. 6 shows

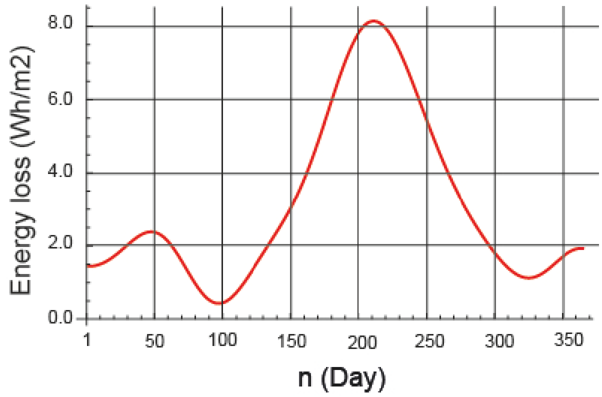

Fig. 3. Daily incident energy loss.

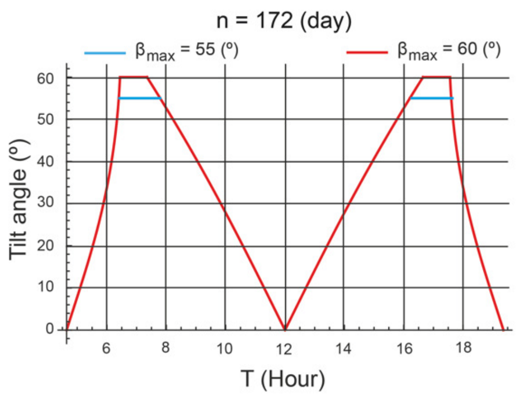

Fig. 4. Tracker operating tilt angles for day n=172.

the behaviour of cos θ_i. Although the better behaviour of the beam component of the actual scenario does not represent a big difference between the two scenarios, it is enough for the actual scenario to obtain better annual results.

Fig. 7 represents only the diffuse component in the actual scenario (red line) and in the $\beta_{\max} = \pm 55(^\circ)$ (blue line) scenario. As can be seen, the $\beta_{\max} = \pm 55(^\circ)$ scenario performs better, but this difference does not compensate for the difference in the beam component. The reflected component has little influence on the incident solar irradiance, due to the low value of the albedo. Therefore, it can be concluded that the scenario of $\beta_{\max} = \pm 55(^\circ)$ slightly favours the diffuse component and the actual scenario favours the beam component. Therefore, a location where the diffuse component is predominant may find that the scenario of $\beta_{\max} = \pm 60(^\circ)$ is not the best.

IV. Conclusions

This paper presents an energy study of the influence of the motion limit of a single-axis horizontal tracker in a PV power plant (Miraflores PV power plant) in Spain. The combination of motion limits defines the study scenarios. As most of the PV power plants in Spain have a motion limit of ± 60 $(^o)$, this is referred to as the actual scenario. Using a Mathematica© code, the annual incident energy and the daily incident energy on the PV field have been calculated. The proposed assessment indicator is the annual incident energy ratio with respect to the actual scenario. In summary, this analysis leads to the following conclusions:

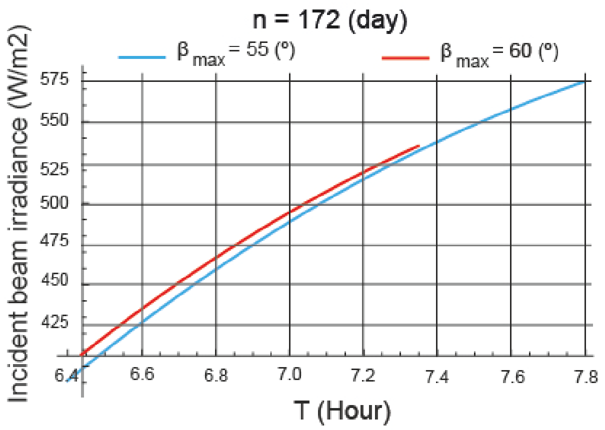

Fig. 5. Comparison of the beam component.

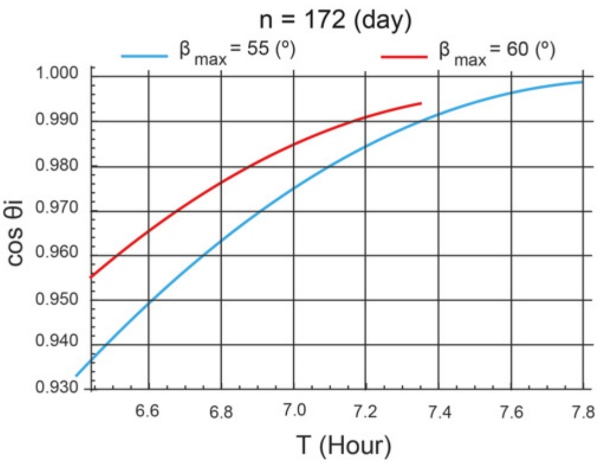

Fig. 6. Comparison of the cos θ_i.

(i) The maximum annual incident energy corresponds to the actual scenario; (ii) Reducing the limit of motion of horizontal single-axis trackers does not involve excessive energy losses. For $\beta_{\max} = \pm 55(^\circ)$ this loss is 0.050%; (iii) The scenario of $\beta_{\max} = \pm 55(^\circ)$ slightly favours the diffuse component and the actual scenario favours the beam component. Therefore, a location where the diffuse component is predominant may find that the scenario of $\beta_{\max} = \pm 60(^\circ)$ is not the best.

We wish to thank Gonvarri Solar Steel [6] for his contribution in this paper.

References

[1] BPIE. 9 Ways to make the energy performance of buildings directive more effective; 2016. Available from: http://bpie.eu/wp-content/uploads/2016/08/EPBD-paper_Eng.pdf, accessed on 27 December 2023.

[2] International Energy Agency (IEA), World energy outlook 2023. https://iea.blob.core.windows.net/assets/ed1e4c42-5726-4269-b801-97b3d32e117c/WorldEnergyOutlook2023.pdf, accessed on 20 February 2024.

[3] IRENA, Future of Solar Photovoltaic: Deployment, Investment, Technology, Grid Integration and Socio-Economic Aspects, International Renewable Energy Agency, 2019, Available from: https://irena.org/-/media/Files/IRENA/Agency/Publication/2019/Nov/IRENA_Future_of_Solar_PV_2019.pdf, accessed on 27 December 2023.

[4] A. Barbón, P. Fortuny Ayuso, L. Bayón, C.A. Silva, A comparative study between racking systems for photovoltaic power systems, Renewable Energy 180 (2021) 424-437.

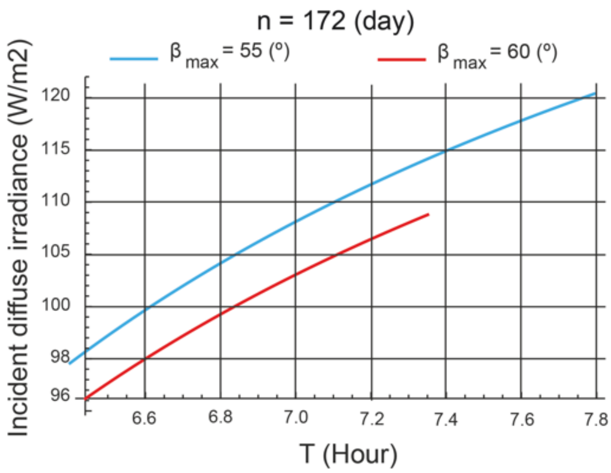

Fig. 7. Comparison of the diffuse component.

[5] S. Martín-Martínez, M. Cañas-Carretón, A. Honrubia-Escribano, E. Gómez-Lázaro, Performance evaluation of large solar photovoltaic power plants in spain, Energy Conversion and Management 183 (2019) 515–28.

[6] Gonvarri Solar Steel. Available from: https://www.gsolarsteel.com/.

[7] A. Barbón, V. Carreira-Fontao, L. Bayón, C.A. Silva, Optimal design and cost analysis of single-axis tracking photovoltaic power plants, Renewable Energy 211 (2023) 626-646.

[8] J.A. Duffie, W.A. Beckman, Solar Engineering of Thermal Processes, 4 ed. New York: John Wiley & Sons; 2013.

[9] J. Antonanzas, R. Urraca, F.J. Martinez-de-Pison, F. Antonanzas, Optimal solar tracking strategy to increase irradiance in the plane of array under cloudy conditions: A study across Europe, Solar Energy 163 (2018) 122-130.

[10] F.J. Casares de la Torre, M. Varo, R. López-Luque, J. Ramírez-Faz, L.M. Fernández-Ahumada, Design and analysis of a tracking / backtracking strategy for PV plants with horizontal trackers after their conversion to agrivoltaic plants, Renewable Energy 187 (2022) 537-550.

[11] A. Barbón, P. Fortuny Ayuso, L. Bayón, J.A. Fernández-Rubiera, Predicting beam and diffuse horizontal irradiance using Fourier expansions, Renewable Energy 154 (2020) 46-57.

[12] A. Barbón, L. Bayón, G. Díaz, C. Bayón-Cueli, Comparative analysis of energy yield of photovoltaic module mounting systems without solar tracker with tilt update for urban applications. In Conference IEEE International Conference on Environmental and Electrical Engineering (EEEIC2022), 2022.

[13] PVGIS, Joint Research Centre (JRC), Available from: https://ec.europa.eu/jrc/en/pvgis, accessed on 10 January 2024.